

UC Davis

UC Davis Previously Published Works

Title

Erythrocytes Are Oxygen-Sensing Regulators of the Cerebral Microcirculation

Permalink

<https://escholarship.org/uc/item/29m3k945>

Journal

Neuron, 91(4)

ISSN

0896-6273

Authors

Wei, Helen Shinru
Kang, Hongyi
Rasheed, Izad-Yar Daniel
[et al.](#)

Publication Date

2016-08-01

DOI

10.1016/j.neuron.2016.07.016

Peer reviewed



Published in final edited form as:

Neuron. 2016 August 17; 91(4): 851–862. doi:10.1016/j.neuron.2016.07.016.

Erythrocytes are oxygen-sensing regulators of the cerebral microcirculation

Helen Shinru Wei¹, Hongyi Kang¹, Izad-Yar Daniel Rasheed², Sitong Zhou³, Nanhong Lou¹, Anna Gershteyn¹, Evan Daniel McConnell¹, Yixuan Wang^{3,4}, Kristopher Emil Richardson⁵, Andre Francis Palmer⁵, Chris Xu⁶, Jiandi Wan³, and Maiken Nedergaard¹

¹Center for Translational Neuromedicine, University of Rochester Medical Center, Rochester, NY 14642

²Department of Neurology, Northwestern University Feinberg School of Medicine, Chicago, IL 60611

³Department of Microsystems Engineering, Rochester Institute of Technology, Rochester, NY 14623

⁴School of Mechanical Engineering, University of Science and Technology, Beijing, 100083, China

⁵William G. Lowrie Department of Chemical & Biomolecular Engineering, The Ohio State University, Columbus, OH 43210

⁶School of Applied & Engineering Physics, Cornell University, Ithaca, NY 14853

Summary

Energy production in the brain depends almost exclusively on oxidative metabolism. Neurons have small energy reserves and require a continuous supply of oxygen (O₂). It is therefore not surprising that one of the hallmarks of normal brain function is the tight coupling between cerebral blood flow and neuronal activity. Since capillaries are embedded in the O₂-consuming neuropil, we have here examined whether activity-dependent dips in O₂ tension drive capillary hyperemia. *In vivo* analyses showed that transient dips in tissue O₂ tension elicit capillary hyperemia. *Ex vivo* experiments revealed that red blood cells (RBCs) themselves act as O₂ sensors that autonomously regulate their own deformability and thereby flow velocity through capillaries in response to physiological decreases in O₂ tension. This observation has broad implications for understanding how local changes in blood flow are coupled to synaptic transmission.

Correspondence: Maiken Nedergaard, Division of Glial Disease and Therapeutics, Center for Translational Neuromedicine, University of Rochester, 601 Elmwood Avenue, Rochester, NY 14642, Phone: 585-273-2868, Fax: 585-275-8126, nedergaard@urmc.rochester.edu or Jiandi Wan, Department of Microsystems Engineering, Rochester Institute of Technology, 160 Lomb Memorial Drive, Rochester, NY 14623, Phone: 585-475-7726, Fax: 585-475-6879, jdween@rit.edu.

Author Contributions

Conceptualization, M.N., J.W., and H.S.W.; Methodology, H.S.W., H.K., I.D.R., N.L., and S.Z.; Software, I.D.R. and H.S.W.; Investigation, M.N., J.W., H.S.W., H.K., N.L., S.Z., Y.W., E.D.M., and A.G.; Resources, A.F.P., K.E.R., and C.X.; Writing – Original Draft, M.N., J.W., and H.S.W.; Writing – Review & Editing, M.N., J.W., H.S.W., S.Z., A.F.P., and I.D.R.; Visualization, M.N., J.W., H.S.W., and S.Z.; Supervision, M.N. and J.W.; Funding Acquisition, M.N. and J.W.

Publisher's Disclaimer: This is a PDF file of an unedited manuscript that has been accepted for publication. As a service to our customers we are providing this early version of the manuscript. The manuscript will undergo copyediting, typesetting, and review of the resulting proof before it is published in its final citable form. Please note that during the production process errors may be discovered which could affect the content, and all legal disclaimers that apply to the journal pertain.

eTOC Blurp

Wei et al. demonstrate a novel mechanism for cerebral capillary blood flow regulation. Erythrocytes can sense and respond to decreases in environmental oxygen tension by autonomously increasing their flow velocities through capillaries and providing a rapid rise in oxygen supply.

Introduction

Neurovascular coupling is a process in which synaptic activity is linked to local changes in cerebral blood flow (Iadecola and Nedergaard, 2007; Kleinfeld et al., 2011). The mechanisms by which neural activity triggers hyperemia have been extensively studied because neurovascular coupling forms the basis for functional brain imaging. In addition, defects in neurovascular coupling may contribute to cognitive decline in neurodegenerative diseases such as Alzheimer disease, as well as in hypertension and stroke (Girouard and Iadecola, 2006). Functional hyperemia can be mediated by a number of compounds, many of which are byproducts of neural activity, including adenosine, nitric oxide (NO), prostaglandin E₂ (PGE₂), potassium ions (K⁺), epoxyeicosatrienoic acids (EETs), and carbon dioxide (CO₂) (Iadecola and Nedergaard, 2007). In addition, functional hyperemia is preceded by a transient decrease in tissue oxygenation (Devor et al., 2011; Lecoq et al., 2011; Parpaleix et al., 2013). Since recent work has documented that functional hyperemia is initiated in microvessels embedded in the oxygen-(O₂) consuming neuropil, we asked whether the initial dip in tissue O₂ tension drives brain capillary hyperemia.

Results

Functional Hyperemia Begins In Capillaries and Is Inhibited When Oxidative Phosphorylation Is Suppressed

To identify the brain region activated by hindlimb stimulation, the exposed cortex was first visualized using intrinsic optical signaling (IOS) followed by high speed two-photon line-scanning to assess red blood cell (RBC) velocities in arterioles and capillaries in the contralateral sensory cortex of lightly sedated mice (Fig. 1A) (Bekar et al., 2012; Takano et al., 2006). Only cortical arterioles and capillaries located in the cortical region that exhibited the largest activity-dependent increase in IOS were analyzed. A comparison of the onset time of stimulation-induced elevation in RBC velocity revealed that capillary RBC velocities (0.67 ± 0.15 s, $n = 65$, 25 mice) increased prior to RBC velocities of upstream arterioles (2.33 ± 0.22 s, $n = 61$, 25 mice) (Fig. 1B), which is consistent with conclusions drawn by a prior study on vascular diameters (Hall et al., 2014). Additional analysis of a subset of connected capillaries and arterioles confirmed that following hindlimb stimulation, the onset of RBC velocity increases in capillaries preceded that of upstream arterioles (Fig. S1A). In these experiments, cortical vascular trees were mapped prior to data collection and corresponding arterioles and capillaries were identified for line-scanning. We also collected line scans orthogonally across vessel widths of arterioles and capillaries. These data showed that arterioles dilated at 2.38 ± 0.37 s, whereas capillary dilation occurred at 2.46 ± 0.22 s after hindlimb stimulation ($n = 53$ – 283 , 15–18 mice) (Fig. 1C). In agreement with a recent

publication, a slight dilation of capillaries was noted, but this occurred concomitant with arteriole dilation and most likely reflected pressure-induced increases in blood flow and/or volume (Hill et al., 2015). Thus, activity-dependent increases in capillary RBC velocities occur prior to both dilations of and RBC velocity increases in upstream arterioles, indicating that capillary hyperemia occurs before arterial hyperemia.

An intraparenchymal dip in partial pressure of oxygen (PO_2) (Yacoub et al., 2001) began at 0.29 ± 0.09 s after hindlimb stimulation (Fig. 1E), similar to previous reports (Lecoq et al., 2011; Parpaleix et al., 2013), and thereby preceded capillary hyperemia by as much as 0.38 seconds. Could the transient dip in tissue PO_2 be responsible for the initial phase of capillary hyperemia? To test this question, we applied sodium cyanide (NaCN), a potent inhibitor of cytochrome c oxidase and thus O_2 utilization, to the exposed cerebral cortex. Initial experiments showed that 0.1 mM NaCN was the highest concentration that did not interfere with excitatory potentials evoked by hindlimb stimulation (Fig. 1D). Applying 0.1 mM NaCN on the pial surface increased resting PO_2 (18.62 ± 2.51 mmHg PO_2 before NaCN, 38.74 ± 4.40 mmHg PO_2 after NaCN, $n = 10$ mice, $p < 0.0001$, paired t-test). NaCN also significantly suppressed stimulation-induced dips in tissue PO_2 though it did not change the onset of the evoked PO_2 dip (Fig. 1E). NaCN reduced the amplitude of capillary hyperemia by 78% ($n = 29-38$, 6–13 mice, $p < 0.001$, t-test) (Fig. 1F), but it did not attenuate activity-evoked penetrating arteriole vasodilation or velocity increases (Fig. 1G–H). This observation is surprising because the release of traditional smooth muscle relaxing mediators of functional hyperemia, including adenosine and K^+ , is potentiated rather than inhibited when oxidative phosphorylation is suppressed (Daval et al., 1980). The fact that NaCN application significantly suppressed capillary hyperemia alone is consistent with the idea that the activity-induced transient dip in tissue PO_2 triggers an increase in local capillary RBC velocity.

PO_2 Dips Are Sufficient to Elicit Capillary Hyperemia

We next asked whether a change in tissue PO_2 , in the absence of sensory activation, is sufficient to trigger capillary hyperemia. To address this question, three structurally different O_2 scavengers, sodium ascorbate, sodium sulfite, or sodium dithionite, were separately microinjected near capillaries in the hindlimb cortex under the guidance of two-photon imaging (Fig. 2A). Ascorbate, sulfite, and dithionite all triggered a rapid decrease in local tissue PO_2 . Similar to activity-dependent responses, tissue PO_2 exhibited a bi-phasic pattern, with an initial transient dip followed by a delayed and long-lasting overshoot (Fig. 2A). Strikingly, RBC velocity increased in nearby capillaries after microinjection of O_2 scavengers, suggesting that tissue oxygenation influences capillary blood flow (Fig. 2B). For more detailed analyses, we focused on sulfite, which is converted to the relatively non-toxic compound, sulfate, after reaction with O_2 . We found that increasing the concentration of sulfite triggered a dose-dependent increase in RBC velocity (Fig. 2C). Sulfite microinjection also caused vasodilation of nearby penetrating arterioles, but the arteriolar vasodilation was delayed relative to sulfite-induced capillary velocity increases (Fig. 2D). Microinjection of the maximal concentration of sulfite (1 M) was not associated with detectable changes in the power spectrum of local field potential (LFP) activity (Fig. 2E). Thus, local application of O_2 scavengers alone in the absence of sensory stimulation triggered hyperemia that closely

resembled activity-dependent hyperemia. Moreover, sulfite elicited capillary hyperemia in both capillaries with and without pericytes in NG2-DsRed mice, suggesting that increases in RBC velocity occurred independent of pericyte presence (Fig. 2F). We defined capillaries with pericytes as capillaries in contact with pericyte cell bodies, and capillaries without pericytes as capillaries lacking contact with pericyte cell bodies. Next, we asked whether it is the depletion of O₂ that directly triggers hyperemia, or whether hyperemia is induced indirectly by release of vasoactive mediators. To systematically address this we tested whether sulfite-elicited capillary hyperemia was reduced by pretreatment with inhibitors of NO production (L-NAME), inhibitors of PGE₂ production (indomethacin), adenosine A1 and A2a receptor antagonists (DPCPX and SCH 58261), or inhibitors of inward rectifying K⁺ channels (barium). Topical application of these inhibitors to the pial surface all failed to suppress sulfite-induced capillary hyperemia (Fig. 2G), indicating that PO₂-induced capillary hyperemia is not dependent on vascular smooth muscle relaxation.

To evaluate the contribution of pericytes to capillary hyperemia, we compared the amplitude and onset time of activity-induced RBC velocity increases of capillaries in contact with pericyte cell bodies with capillaries lacking contact with pericyte cell bodies in NG2-DsRed reporter mice. The baseline capillary diameter adjacent to the cell bodies of NG2-DsRed pericytes did not differ from segments of capillaries not in contact with pericyte cell bodies (Fig. S2A). We found that activity-evoked capillary hyperemia was unaffected by the presence or absence of an adjacent pericyte cell body. Capillary RBC velocity began at 0.71 ± 0.35 s in capillaries with pericytes (n = 28, 5 mice) and at 0.66 ± 0.22 s in capillaries without pericytes (n = 31, 5 mice) (Fig. S2B). Next, we evaluated pericyte expression of actin in mouse cortex using phalloidin staining of F-actin as well as α -smooth muscle actin (α -SMA) immunolabeling in fixed sections. Similar to prior studies, we defined the penetrating vessel as the zeroth branch order vessel, with subsequent branches labeled using increasing branch order numbers (Hall et al., 2014; Hill et al., 2015; Kornfield and Newman, 2014). Quantification confirmed that vessels beyond the third branch order were largely phalloidin and α -SMA negative (only 1.4% of vessels fourth order or higher, averaging 4.0 μ m in diameter, were phalloidin and/or α -SMA positive, n = 49 vessels from 9 mice). In contrast, vessel branches zero to three were largely phalloidin and/or α -SMA positive (22–100% actin-positive, ranging from 5.4 to 13.3 μ m in diameter, n = 12–25 vessels from 9 mice) (Fig. S2C). Only ~30% of DsRed⁺ pericyte cell bodies along branches one to three were actin-positive (Fig. S2D–E). These observations are in agreement with a recent study showing that smooth muscle actin is expressed by arterioles but not capillary mural cells in mouse and human neocortex (Hill et al., 2015). Hill et al. also showed that unlike smooth muscle actin-positive arterioles, pericyte-covered capillaries do not constrict or dilate in response to stimulation.

An important detail for validation of our *in vivo* analysis was our finding that 100% of DsRed-positive cells were PDGFR β -positive and conversely that 100% of PDGFR β -positive cells were DsRed-positive in NG2-DsRed reporter mice (Fig. S2F). In addition, DsRed-positive perivascular cells in NG2-DsRed reporter mice stained positively for desmin and CD13 in immunohistochemical slices (Fig. S2G). Therefore, capillaries identified as with or without pericytes during *in vivo* imaging of NG2-DsRed reporter mice were properly

categorized, as PDGFR β , desmin, and CD13 are pericyte-specific markers (Armulik et al., 2011).

AMPA Receptor Activity Modulates Capillary RBC Velocity

The velocity by which RBCs pass through capillaries is highly variable (Chaigneau et al., 2003; Kleinfeld et al., 1998; Stefanovic et al., 2008). Based on the observation of a tight coupling between postsynaptic AMPA receptor activity and tissue PO₂ (Enager et al., 2009; Mathiesen et al., 2011), as well as our observation that NaCN inhibits both evoked PO₂ dips and capillary hyperemia (Fig. 1E–F) while microinjection of O₂ scavengers induces capillary hyperemia (Fig. 2B), we asked whether the ever-changing pattern of synaptic activity contributes to spontaneous fluctuations in capillary RBC velocity.

The AMPA receptor antagonist, CNQX (200 μ M) was topically applied to the cerebral cortex and its effect on baseline (unstimulated) LFPs, PO₂, and capillary RBC velocity was assessed. As a measure of baseline variability, we compared the standard deviation of LFPs, PO₂, and capillary RBC velocity before and after application of CNQX (Fig. 3A–C). As expected, CNQX potently suppressed both the power and the standard deviation (SD) of baseline LFPs (Fig. 3A). Baseline PO₂ levels also exhibited a significant increase (52.6% increase) and the variability of baseline PO₂ was reduced (45.0% suppression of SD by CNQX) (Fig. 3B). Baseline capillary RBC velocity decreased by 25.7% and interestingly, the SD of RBC velocity fluctuations also fell significantly in response to CNQX (26.7% suppression by CNQX) (Fig. 3C), suggesting that AMPA-receptor mediated PO₂ dips in part contribute to the variability of capillary RBC velocity at rest. Prior analyses have shown that cardiac- and respiration-dependent pulsatile blood flow is also in part responsible for the high variability in baseline capillary RBC velocities (Santisakultarm et al., 2012). Of note, baseline arterial diameter remained unchanged after addition of CNQX (Fig. 3D). To extend the analysis to include capillary functional hyperemia, we next compared responses to hindlimb stimulation before and after addition of CNQX. As expected, CNQX produced a dramatic decrease in excitatory potentials and PO₂ dip amplitudes evoked by a 2-second hindlimb stimulation (81.0% and 90.1% suppression by CNQX, respectively) (Fig. 3E–F). Consistent with the key role of AMPA receptor activation in functional hyperemia, CNQX significantly delayed the onset and suppressed the amplitude of capillary RBC velocity increases in response to hindlimb stimulation (75.0% suppression by CNQX) (Fig. 3G). Figures 3H–I compare the relative power by which blockade of AMPA receptors suppressed spontaneous fluctuations and stimulation-dependent changes in LFPs, PO₂, and capillary RBC velocity. Of note, inhibition of NMDA receptors (AP5, 500 μ M) did not have a significant effect on capillary hyperemia (Fig. S3). This observation is consistent with the idea that excitatory transmission is primarily the result of AMPA receptor activation in the sensory cortex (Hoffmeyer et al., 2007; Self et al., 2012).

Together, these results suggest that O₂-consuming synaptic activity is partly responsible for the variability of cortical capillary RBC velocities during resting conditions, and primarily responsible for the initiation of activity-dependent capillary hyperemia.

Oxygen Depletion Alone Is Sufficient to Increase RBC Velocity *ex vivo*

The observation that microinjection of O₂ scavengers induced pericyte- and vasoactive mediator-independent capillary hyperemia led us to hypothesize that O₂ tension itself, independent of the neurovascular unit, can control RBC deformation and thus RBC flow through capillaries. To test this idea in the absence of the neurovascular unit, we turned to an *ex vivo* assessment of the effect of oxygenation on RBC flow through an artificial capillary. We employed a microfluidic device in which isolated human RBCs pass through a narrow flow channel (Fig. 4A) (Abkarian et al., 2006; Cinar et al., 2015; Wan et al., 2011; Wan et al., 2008). This approach allowed an evaluation of RBC velocity in the absence of the cellular components of the neurovascular unit, i.e. endothelial cells, pericytes, and astrocytes (Petzold and Murthy, 2011). Since the capillary lumen is considerably smaller than RBC diameters, RBC deformability is a major determinant of the speed by which the RBC passes through a capillary (Chaigneau et al., 2003). A microfluidic device made of polydimethylsiloxane (PDMS) was submerged in a chamber containing sodium sulfite, an O₂ scavenger. Since PDMS is O₂, but not H₂O permeable, the chamber functioned as a sink for O₂ (Fig. 4A). A colorimetric calibration, based on adding the O₂-sensing dye, tris(2,2'-bipyridyl)dichlororuthenium(II) hexahydrate, to deionized (DI) water showed that PO₂ in the flow channel was an inverse function of the sulfite concentration (0 to 2 M) (Fig. 4B). Remarkably, the velocity of RBCs flowing through the channel increased as a function of O₂ depletion, indicating that brief deoxygenation alone can affect the mechanical properties of RBCs (Fig. 4B–C). The O₂-dependent increase in RBC velocity was observed when RBCs were resuspended in either plasma or PBS (Fig. 4C). Because PO₂ in capillaries is highly variable and can range from ~5–95 mmHg but tends to be on the lower end of that range within true microvessels (Kasischke et al., 2011; Parpaleix et al., 2013; Sakadzic et al., 2014), we focused on the effects of relatively lower PO₂. In these experiments, the PBS was first purged with N₂ until the PO₂ reached 34 mmHg, approximating normal brain PO₂ (Jaeger et al., 2005). Similar to above, RBCs were driven through a microfluidic chamber immersed in a sulfite sink (0 to 1 M) and colorimetrically calibrated (Fig. 4B). This analysis showed that at a relatively lower range of O₂ tension, RBC velocities became more sensitive to surrounding changes in PO₂ ($p < 0.001$, t-test with Bonferroni test, compared to PBS without N₂ purging and plasma) (Fig. 4C–D). Interestingly however, increasing the O₂ from 21% to 100% (or from PO₂ ~160 mmHg to ~760 mmHg) failed to alter RBC velocity in the microfluidic capillary (1.000 normalized velocity in 21% vs 0.998 normalized velocity in 100% O₂, $n = 9–19$, $p > 0.05$, t-test), consistent with the notion that at superphysiologic PO₂, hemoglobin continues to be maximally saturated with O₂ and RBCs reach the limit of their ability to bind additional O₂ and respond with velocity changes. Classical studies have shown that in response to deoxygenation and/or mechanical stress, RBCs release ATP which activates endothelial cell purinergic receptors (P₂YR1s) resulting in NO release. In turn, NO or other endothelium-dependent vasodilators increase blood flow in hypoxic tissues via arterial smooth muscle relaxation (Chen et al., 2014; Ellsworth et al., 2009; Jia et al., 1996). RBCs may also directly release NO from S-nitroso-Hb upon deoxygenation (Jensen, 2009). However, we found that the PO₂-elicited increase in RBC flow velocity was not a result of direct ATP or NO release. Exposing RBCs to the ATP-degrading enzyme apyrase (40 U/mL) or the NO synthase inhibitor L-NAME (3 mM) did not affect PO₂-induced elevations in RBC velocity (Fig. 4D), in accordance with the *in vivo* observation that L-NAME failed to

suppress capillary hyperemia (Fig. 2G). In addition, CNQX had no effect on PO₂-induced increases in RBC velocity through the microfluidic channel (Fig. 4D). When RBCs were treated with K⁺ channel inhibitors (4-aminopyridine (4-AP, non-selective voltage-dependent K⁺ channel blocker, 1 mM), charybdotoxin (Ca²⁺-activated voltage-gated K⁺ channel blocker, 100 nM), or iberiotoxin (large-conductance Ca²⁺-activated K⁺ channel blocker, 100 nM)), however, the sensitivity of RBC velocity to PO₂ changes decreased (Fig. 4E), suggesting that K⁺ flux across the membrane plays a role in the velocity of RBC flow in capillaries. As a negative control, RBCs were treated with diamide, which stiffens the RBC membrane by crosslinking the cytoskeletal spectrin network (Fischer et al., 1978; Wan et al., 2008). The flow velocity of diamide-exposed RBCs was unaffected by PO₂, supporting the notion that the PO₂-induced increase in RBC flow velocity is due to increased deformability of the RBC membrane (Fig. 4D).

To directly test whether RBC deformability is controlled by PO₂, we assessed the shear-induced deformability of RBCs flowing in a relatively large-sized microfluidic channel containing a segment of constriction (width = 20 μm) (Fig. 4F). The shear-induced deformability of RBCs was characterized by the elongation index D_L/D_W where D_L and D_W represented the length and thickness of a RBC flowing through the constriction, respectively (adapted from (Forsyth et al., 2010; Mohandas et al., 1980)). We found that the elongation of RBCs in response to shear stress increased as PO₂ decreased, demonstrating that RBCs are more flexible in lower PO₂ conditions (Fig. 4G). The dependence of RBC deformability on PO₂ was significantly diminished when diamide was added (Fig. 4G). RBCs treated with the K⁺ channel blockers 4-AP (1 mM), charybdotoxin (100 nM), or iberiotoxin (100 nM) also exhibited reduced sensitivity to PO₂ changes compared to controls (Fig. 4H). These data show that lowering PO₂ increases RBC deformability and thereby the velocity by which RBCs pass through a narrow *ex vivo* capillary lacking endothelial cells, pericytes, and astrocytes. Exposure to K⁺ channel inhibitors reduced the deformability of RBCs and thus the potency by which PO₂ increased RBC flow velocity. This latter observation is consistent with prior studies documenting that a decrease in cell volume mediated by K⁺ efflux and water loss may play a role in permitting RBC deformation during the shear stress associated with squeezing through a narrow capillary (Cinar et al., 2015).

Exchanging RBCs For An O₂-Carrying Blood Substitute Suppresses Functional Hyperemia *in vivo*

Our *ex vivo* data suggest that RBCs autonomously regulate their own velocities through capillaries in response to changes in surrounding PO₂ tension. If this finding is relevant *in vivo*, we would expect that *in vivo* capillary hyperemia is suppressed when RBCs are replaced by an acellular hemoglobin-based O₂ carrier (HBOC). To meticulously test whether RBCs are required for activity-dependent capillary hyperemia, we partially exchanged the blood in our mouse model with a synthetic HBOC, i.e. polymerized hemoglobin (PolyHb) (Baek et al., 2012; Zhou et al., 2011). We were able to decrease the hematocrit by $80.3 \pm 0.5\%$ (10.55 ± 0.11 vs. $2.08 \pm 0.046 \times 10^6$ cells per μL) by gradually replacing RBCs with PolyHb. Mixing PolyHb with whole blood did not alter blood viscosity (Fig. 5A). PolyHb blood exchange did not alter resting cortical PO₂, sensory-induced dips in PO₂ (Fig. 5B), or sensory-evoked electrical activity (evoked LFP 10 Hz power was 0.017 ± 0.0085 mV² in

control mice and $0.015 \pm 0.0064 \text{ mV}^2$ in PolyHb mice, $p > 0.05$, t-test). It did, however, delay the onset time and reduce the amplitude of activity-dependent capillary hyperemia (Fig. 5C–D). Basal cortical arteriole diameters were unchanged but evoked arteriole vasodilation was reduced with PolyHb (Fig. 5E). With an insufficient RBC population, capillary hyperemia may be primarily driven by upstream arteriole vasodilation.

How does hyperoxygenation affect the microcirculation? Breathing 100% O_2 elevated baseline cortical PO_2 from ~ 25 to ~ 50 mmHg (Jaeger et al., 2005), without causing significant changes in the evoked PO_2 dip (Fig. 5F). Basal capillary RBC velocities were reduced while basal arteriole diameters and capillary hyperemia were unchanged (Fig. 5G–H). Hence, both the *ex vivo* and *in vivo* observations provide strong support for the notion that deoxygenation-mediated changes in erythrocyte deformability drive capillary hyperemia.

Discussion

Despite the uncontested tight linkage between neural activity and vascular responses, the question of what drives functional hyperemia is still debated. In principle, a mechanism sensing depletion of an energy substrate (O_2 or glucose) or alternatively the release of vasoactive mediators (NO, PGE_2 , ATP, adenosine, K^+ , and other molecules) could drive activity-dependent increases in blood flow. In this work, we took advantage of the discovery that functional hyperemia is initiated in microvessels rather than in arterioles (Hall et al., 2014). We confirmed that capillary RBC velocity increases 1–2 seconds prior to arterial hyperemia, but similar to a recent study (Hill et al., 2015) failed to identify pericytes as the principal regulator of capillary hyperemia. Several experimental findings presented here implicate the transient PO_2 dip in the initiation of the activity-dependent increase in capillary perfusion via a mechanism independent of the release of vasoactive agents and smooth muscle relaxation, including: (1) Capillary functional hyperemia was suppressed when oxidative metabolism was inhibited by local application of NaCN. Not only does this observation support the notion that PO_2 regulates capillary perfusion, but it also indirectly provides evidence against a central role of vasoactive mediators in initiating functional hyperemia, since adenosine, lactate, and K^+ release are all increased when oxidative metabolism is inhibited (Daval et al., 1980). (2) The AMPA receptor blocker CNQX suppressed the spontaneous fluctuations in resting PO_2 and capillary RBC velocity by 45.0% and 26.7%, respectively, indicating that AMPA receptor activity in part drives spontaneous changes in O_2 tension and capillary RBC flow. Moreover, activity-induced PO_2 dips (90.1%) and capillary hyperemia (75.0%) were both potently suppressed by CNQX. (3) Microinjection of O_2 scavengers induced capillary hyperemia in the absence of an increase in neural activity. The hyperemia induced by local scavenging of O_2 was not suppressed by antagonists of adenosine A1 and A2A receptors or inhibitors of K^+ channels, NO and PGE_2 production, or O_2 consumption (NaCN). (4) *Ex vivo* quantification of the velocity of RBCs moving through a microfluidic channel under strict PO_2 control showed that RBC velocity increased as a direct function of physiologically relevant decreases in PO_2 . Transient manipulation of PO_2 within the range of 0–160 mmHg directly controlled not only the velocity by which RBCs traveled through a narrow synthetic channel in the absence of endothelial cells, pericytes, and astrocytes, but also RBC deformability in response to shear

stress. In contrast, elevation of PO₂ (100% O₂) considerably past physiologic levels failed to decrease RBC velocity beyond what was observed in room air (~21% O₂). (5) Partial replacement of intravascular RBCs with a synthetic RBC-free blood substitute *in vivo* showed that lowering the hematocrit by ~80% was associated with a significant reduction in activity-dependent capillary hyperemia. Together, these observations provide evidence to support the novel concept that RBCs are not only sensors of PO₂ but can also regulate their deformability and thereby the velocity with which they pass through capillaries in response to transient drops in tissue oxygenation.

The effect of PO₂ on RBC deformability is debated, possibly because most past studies were based on indirect measurements that have not been readily reproducible (Kim et al., 2015; Martindale and McKay, 1995; Yoon et al., 2009). To our knowledge no prior studies have directly quantified changes in RBC velocity and deformability in response to *transient* changes in PO₂. The data presented here using an *ex vivo* microfluidic approach demonstrate a direct relationship between RBC velocity and deformability elicited by transient decreases in PO₂.

Deoxygenation of RBCs leads to displacement of ankyrin from band 3, resulting in release of the spectrin/actin cytoskeleton from the cell membrane (Stefanovic et al., 2013). The weakening of membrane-cytoskeletal interactions has been proposed to be beneficial to blood flow during brief periods of deoxygenation (Stefanovic et al., 2013) and may contribute to increased RBC deformability during drops in PO₂. Prior studies in peripheral tissues have shown that RBCs can induce hyperemia but pointed to a mechanism that involves ATP release from RBCs (under shear-induced deformation and/or hypoxia), which triggers endothelial cell NO production that subsequently dilates arteries by hyperpolarizing vascular smooth muscle cells (Ellsworth et al., 2009). Our microfluidic chamber experiments showing that lowering PO₂ in the absence of the neurovascular unit increased isolated RBC velocity, coupled with the finding that L-NAME (an inhibitor of NO synthase) had no effect on capillary hyperemia, argue against a significant contribution from this paracellular signaling mechanism. Furthermore, PO₂-induced arteriole dilation was delayed relative to PO₂-induced capillary blood flow increases, mimicking hyperemia elicited by sensory input and signifying that arteriole vasodilation is not the primary driver of PO₂-dependent capillary hyperemia. Previously, the existence of an O₂-sensing mechanism has been questioned based on the finding that regional functional hyperemia persisted in hyperbaric hyperoxia (Lindauer et al., 2010). We here confirmed that capillary hyperemia was preserved in hyperoxia but extended the analysis to show that activity-induced PO₂ dips persisted during hyperoxic conditions. Thus, hyperoxia did not suppress either activity-induced PO₂ dips or capillary hyperemia. Additionally, inhibiting metabolic O₂ consumption by application of cyanide blocked both activity-dependent dips in PO₂ and capillary hyperemia irrespective of the baseline tissue PO₂. Collectively, these sets of data suggest that it is the transient PO₂ dip rather than baseline PO₂ that triggers capillary hyperemia. This conclusion is further supported by our *ex vivo* observation that RBC velocity in the microfluidic device increased in response to PO₂ reductions across a wide range of physiological PO₂ levels (0–160 mmHg).

It is important to note that functional hyperemia outlasted the dip in PO₂. Accordingly, only the very initial phase (< 1.5 s) of capillary hyperemia that precedes arterial dilation is driven by activity-induced dips in PO₂. The initial capillary response during functional hyperemia may serve as the rapid phase of hyperemia that supplies active neurons with immediately available O₂. The delayed and sustained hyperemic phase is most likely powered by the slower dilation of upstream arterioles and serves to prevent a prolonged drop in oxygenation at tissue located more remotely from arterioles and proximal capillaries (Devor et al., 2011; Leithner and Royl, 2014). It is unclear whether PO₂-mediated rapid capillary hyperemia directly causes delayed arteriole vasodilation, as it has been shown that release of vasoactive agents from both interneurons and astrocytes can trigger arteriole dilation (Cauli and Hamel, 2010; Takano et al., 2006). Capillary hyperemia and arteriole hyperemia may have independent regulatory mechanisms that work in a concerted manner to optimize blood supply. Alternatively, the delayed dilation of upstream arterioles may be a consequence of PO₂-induced rapid capillary hyperemia, mediated by the propagation of Ca²⁺ signals along the neurovascular unit (Fig. 6). If so, it is interesting to speculate whether the impaired vasoreactivity observed in various diseases and in aging is a consequence of impaired PO₂-mediated capillary hyperemia. Future studies can address the relationship between capillary hyperemia and delayed arteriole dilation. Further experiments can also assess sensory-evoked capillary hyperemia in awake behaving mice.

Functional hyperemia is an integrated response that tightly couples O₂ consumption with O₂ supply. Here we show that both spontaneous and activity-induced dips in tissue PO₂ drive the earliest phase of capillary hyperemia. Furthermore, PO₂ directly controls the velocity by which RBCs transit through a narrow channel in a microfluidic device. Thus, RBCs may themselves serve as autonomous regulators of capillary perfusion that operate independently of the neurovascular unit and the release of vasoactive molecules. The idea that erythrocytes – the major suppliers of O₂ – function not only as O₂ carriers but also as O₂ sensors and regulators of capillary blood flow provides a simple, yet swift and precise mechanism for controlling the cerebral microcirculation.

Experimental Procedures

Animals

C57Bl6 mice (25–30 g, 8–12 weeks old, The Jackson Laboratory) and NG2-DsRed mice (Tg(Cspg4-DsRed.T1)1Akik/J, RRID: IMSR_JAX:008241) (Zhu et al., 2008) on a C57Bl6 background of either sex were utilized. Mice were prepared for *in vivo* imaging as described previously (Bekar et al., 2008; Ding et al., 2013; Wang et al., 2006; Xie et al., 2013) and in the Supplemental Experimental Procedures.

Physiological manipulations and measurements

Physiological manipulations and measurements were performed as previously described (Baek et al., 2012; Bekar et al., 2012; Kasischke et al., 2011; Takano et al., 2007; Vazquez et al., 2011; Xie et al., 2013; Zhou et al., 2011) and in the Supplemental Experimental Procedures.

Microfluidic device and RBC imaging

Microfluidic device construction and human RBC imaging were performed as previously described (Duffy et al., 1998; Wan et al., 2011; Wan et al., 2008) and in the Supplemental Experimental Procedures.

Intrinsic optical signal and two-photon imaging

Intrinsic optical signaling (IOS), two-photon imaging, and immunofluorescence imaging were performed as previously described (Armulik et al., 2011; Bekar et al., 2012) and in the Supplemental Experimental Procedures.

Statistics

All data were expressed as mean \pm SEM. Normality of the data was evaluated with the Shapiro-Wilk test, and non-parametric tests were used when normality was not assumed. A Student's t-test or Mann-Whitney test was used to compare two groups. A one-way ANOVA with a Bonferroni's multiple comparison test or a Kruskal-Wallis test with a Dunn's multiple comparison test was used to compare multiple groups. A paired t-test or Wilcoxon matched-pairs signed rank test was used for pairwise comparisons. $p < 0.05$ was considered significant.

Supplementary Material

Refer to Web version on PubMed Central for supplementary material.

Acknowledgments

This study was supported by the NIH/NINDS. We thank Takahiro Takano, Lulu Xie, Wei Song, Priyanka Pillai, Prishanya Pillai, and Jordana Schmierer for expert technical assistance, and Dan Xue for assistance with illustrations.

References

- Abkarian M, Faivre M, Stone HA. High-speed microfluidic differential manometer for cellular-scale hydrodynamics. *Proceedings of the National Academy of Sciences of the United States of America*. 2006; 103:538–542. [PubMed: 16407104]
- Armulik A, Genove G, Betsholtz C. Pericytes: developmental, physiological, and pathological perspectives, problems, and promises. *Developmental cell*. 2011; 21:193–215. [PubMed: 21839917]
- Baek JH, Zhou Y, Harris DR, Schaer DJ, Palmer AF, Buehler PW. Down selection of polymerized bovine hemoglobins for use as oxygen releasing therapeutics in a guinea pig model. *Toxicological sciences: an official journal of the Society of Toxicology*. 2012; 127:567–581. [PubMed: 22416071]
- Bekar L, Libionka W, Tian GF, Xu Q, Torres A, Wang X, Lovatt D, Williams E, Takano T, Schnermann J, et al. Adenosine is crucial for deep brain stimulation-mediated attenuation of tremor. *Nature medicine*. 2008; 14:75–80.
- Bekar LK, Wei HS, Nedergaard M. The locus coeruleus-norepinephrine network optimizes coupling of cerebral blood volume with oxygen demand. *Journal of cerebral blood flow and metabolism: official journal of the International Society of Cerebral Blood Flow and Metabolism*. 2012; 32:2135–2145.
- Cauli B, Hamel E. Revisiting the role of neurons in neurovascular coupling. *Frontiers in neuroenergetics*. 2010; 2:9. [PubMed: 20616884]
- Chaigneau E, Oheim M, Audinat E, Charpak S. Two-photon imaging of capillary blood flow in olfactory bulb glomeruli. *Proceedings of the National Academy of Sciences of the United States of America*. 2003; 100:13081–13086. [PubMed: 14569029]

- Chen BR, Kozberg MG, Bouchard MB, Shaik MA, Hillman EM. A critical role for the vascular endothelium in functional neurovascular coupling in the brain. *J Am Heart Assoc.* 2014; 3:e000787. [PubMed: 24926076]
- Cinar E, Zhou S, DeCoursey J, Wang Y, Waugh RE, Wan J. Piezo1 regulates mechanotransductive release of ATP from human RBCs. *Proceedings of the National Academy of Sciences of the United States of America.* 2015; 112:11783–11788. [PubMed: 26351678]
- Daval JL, Barberis C, Gayet J. Release of [¹⁴C]adenosine derivatives from superfused synaptosome preparations. Effects of depolarizing agents and metabolic inhibitors. *Brain research.* 1980; 181:161–174. [PubMed: 7350951]
- Devor A, Sakadzic S, Saisan PA, Yaseen MA, Roussakis E, Srinivasan VJ, Vinogradov SA, Rosen BR, Buxton RB, Dale AM, Boas DA. “Overshoot” of O₂ is required to maintain baseline tissue oxygenation at locations distal to blood vessels. *The Journal of neuroscience: the official journal of the Society for Neuroscience.* 2011; 31:13676–13681. [PubMed: 21940458]
- Ding F, O’Donnell J, Thrane AS, Zeppenfeld D, Kang H, Xie L, Wang F, Nedergaard M. alpha1-Adrenergic receptors mediate coordinated Ca²⁺ signaling of cortical astrocytes in awake, behaving mice. *Cell calcium.* 2013; 54:387–394. [PubMed: 24138901]
- Duffy DC, McDonald JC, Schueller OJ, Whitesides GM. Rapid Prototyping of Microfluidic Systems in Poly(dimethylsiloxane). *Analytical chemistry.* 1998; 70:4974–4984. [PubMed: 21644679]
- Ellsworth ML, Ellis CG, Goldman D, Stephenson AH, Dietrich HH, Sprague RS. Erythrocytes: oxygen sensors and modulators of vascular tone. *Physiology.* 2009; 24:107–116. [PubMed: 19364913]
- Enager P, Piilgaard H, Offenhauser N, Kocharyan A, Fernandes P, Hamel E, Lauritzen M. Pathway-specific variations in neurovascular and neurometabolic coupling in rat primary somatosensory cortex. *Journal of cerebral blood flow and metabolism: official journal of the International Society of Cerebral Blood Flow and Metabolism.* 2009; 29:976–986.
- Fischer TM, Haest CW, Stohr M, Kamp D, Deuticke B. Selective alteration of erythrocyte deformability by SH-reagents: evidence for an involvement of spectrin in membrane shear elasticity. *Biochimica et biophysica acta.* 1978; 510:270–282. [PubMed: 667045]
- Forsyth AM, Wan J, Ristenpart WD, Stone HA. The dynamic behavior of chemically “stiffened” red blood cells in microchannel flows. *Microvascular research.* 2010; 80:37–43. [PubMed: 20303993]
- Girouard H, Iadecola C. Neurovascular coupling in the normal brain and in hypertension, stroke, and Alzheimer disease. *J Appl Physiol (1985).* 2006; 100:328–335. [PubMed: 16357086]
- Hall CN, Reynell C, Gesslein B, Hamilton NB, Mishra A, Sutherland BA, O’Farrell FM, Buchan AM, Lauritzen M, Attwell D. Capillary pericytes regulate cerebral blood flow in health and disease. *Nature.* 2014; 508:55–60. [PubMed: 24670647]
- Hill R, Toing L, Yan P, Murkinati S, Gupta S, Grutzendler J. Regional Blood Flow in the Normal and Ischemic Brain Is Controlled by Arteriolar Smooth Muscle Cell Contractility and Not by Capillary Pericytes. *Neuron.* 2015; 87:1–16. [PubMed: 26139363]
- Hoffmeyer HW, Enager P, Thomsen KJ, Lauritzen MJ. Nonlinear neurovascular coupling in rat sensory cortex by activation of transcallosal fibers. *Journal of cerebral blood flow and metabolism: official journal of the International Society of Cerebral Blood Flow and Metabolism.* 2007; 27:575–587.
- Iadecola C, Nedergaard M. Glial regulation of the cerebral microvasculature. *Nature neuroscience.* 2007; 10:1369–1376. [PubMed: 17965657]
- Jaeger M, Soehle M, Meixensberger J. Brain tissue oxygen (PtiO₂): a clinical comparison of two monitoring devices. *Acta Neurochir Suppl.* 2005; 95:79–81. [PubMed: 16463825]
- Jensen FB. The dual roles of red blood cells in tissue oxygen delivery: oxygen carriers and regulators of local blood flow. *The Journal of experimental biology.* 2009; 212:3387–3393. [PubMed: 19837879]
- Jia L, Bonaventura C, Bonaventura J, Stamler JS. S-nitrosohaemoglobin: a dynamic activity of blood involved in vascular control. *Nature.* 1996; 380:221–226. [PubMed: 8637569]
- Kasischke KA, Lambert EM, Panepento B, Sun A, Gelbard HA, Burgess RW, Foster TH, Nedergaard M. Two-photon NADH imaging exposes boundaries of oxygen diffusion in cortical vascular

- supply regions. *Journal of cerebral blood flow and metabolism: official journal of the International Society of Cerebral Blood Flow and Metabolism*. 2011; 31:68–81.
- Kim J, Le H, Shin S. Advances in the measurement of red blood cell deformability: A brief review. *Journal of Cellular Biotechnology*. 2015; 1:63–79.
- Kleinfeld D, Blinder P, Drew PJ, Driscoll JD, Muller A, Tsai PS, Shih AY. A guide to delineate the logic of neurovascular signaling in the brain. *Frontiers in neuroenergetics*. 2011; 3:1. [PubMed: 21559095]
- Kleinfeld D, Mitra PP, Helmchen F, Denk W. Fluctuations and stimulus-induced changes in blood flow observed in individual capillaries in layers 2 through 4 of rat neocortex. *Proceedings of the National Academy of Sciences of the United States of America*. 1998; 95:15741–15746. [PubMed: 9861040]
- Kornfield TE, Newman EA. Regulation of blood flow in the retinal trilaminar vascular network. *The Journal of neuroscience: the official journal of the Society for Neuroscience*. 2014; 34:11504–11513. [PubMed: 25143628]
- Lecoq J, Parpaleix A, Roussakis E, Ducros M, Goulam Houssen Y, Vinogradov SA, Charpak S. Simultaneous two-photon imaging of oxygen and blood flow in deep cerebral vessels. *Nature medicine*. 2011; 17:893–898.
- Leithner C, Royl G. The oxygen paradox of neurovascular coupling. *Journal of cerebral blood flow and metabolism: official journal of the International Society of Cerebral Blood Flow and Metabolism*. 2014; 34:19–29.
- Lindauer U, Leithner C, Kaasch H, Rohrer B, Foddiss M, Fuchtemeier M, Offenhauser N, Steinbrink J, Royl G, Kohl-Bareis M, Dirnagl U. Neurovascular coupling in rat brain operates independent of hemoglobin deoxygenation. *Journal of cerebral blood flow and metabolism: official journal of the International Society of Cerebral Blood Flow and Metabolism*. 2010; 30:757–768.
- Martindale VE, McKay K. Hyperbaric oxygen treatment of dogs has no effect on red cell deformability but causes an acute fluid shift. *Physiological chemistry and physics and medical NMR*. 1995; 27:45–53.
- Mathiesen C, Caesar K, Thomsen K, Hoogland TM, Witgen BM, Brazhe A, Lauritzen M. Activity-dependent increases in local oxygen consumption correlate with postsynaptic currents in the mouse cerebellum in vivo. *The Journal of neuroscience: the official journal of the Society for Neuroscience*. 2011; 31:18327–18337. [PubMed: 22171036]
- Mohandas N, Clark MR, Jacobs MS, Shohet SB. Analysis of factors regulating erythrocyte deformability. *The Journal of clinical investigation*. 1980; 66:563–573. [PubMed: 6156955]
- Parpaleix A, Goulam Houssen Y, Charpak S. Imaging local neuronal activity by monitoring PO(2) transients in capillaries. *Nature medicine*. 2013; 19:241–246.
- Petzold GC, Murthy VN. Role of astrocytes in neurovascular coupling. *Neuron*. 2011; 71:782–797. [PubMed: 21903073]
- Sakadzic S, Mandeville ET, Gagnon L, Musacchia JJ, Yaseen MA, Yucel MA, Lefebvre J, Lesage F, Dale AM, Eikermann-Haerter K, et al. Large arteriolar component of oxygen delivery implies a safe margin of oxygen supply to cerebral tissue. *Nature communications*. 2014; 5:5734.
- Santisakultarm TP, Cornelius NR, Nishimura N, Schafer AI, Silver RT, Doerschuk PC, Olbricht WL, Schaffer CB. In vivo two-photon excited fluorescence microscopy reveals cardiac- and respiration-dependent pulsatile blood flow in cortical blood vessels in mice. *American journal of physiology Heart and circulatory physiology*. 2012; 302:H1367–1377. [PubMed: 22268102]
- Self MW, Kooijmans RN, Super H, Lamme VA, Roelfsema PR. Different glutamate receptors convey feedforward and recurrent processing in macaque V1. *Proceedings of the National Academy of Sciences of the United States of America*. 2012; 109:11031–11036. [PubMed: 22615394]
- Stefanovic B, Hutchinson E, Yakovleva V, Schram V, Russell JT, Belluscio L, Koretsky AP, Silva AC. Functional reactivity of cerebral capillaries. *Journal of cerebral blood flow and metabolism: official journal of the International Society of Cerebral Blood Flow and Metabolism*. 2008; 28:961–972.
- Stefanovic M, Puchulu-Campanella E, Kodippili G, Low PS. Oxygen regulates the band 3-ankyrin bridge in the human erythrocyte membrane. *The Biochemical journal*. 2013; 449:143–150. [PubMed: 23013433]

- Takano T, Tian GF, Peng W, Lou N, Libionka W, Han X, Nedergaard M. Astrocyte-mediated control of cerebral blood flow. *Nature neuroscience*. 2006; 9:260–267. [PubMed: 16388306]
- Takano T, Tian GF, Peng W, Lou N, Lovatt D, Hansen AJ, Kasischke KA, Nedergaard M. Cortical spreading depression causes and coincides with tissue hypoxia. *Nature neuroscience*. 2007; 10:754–762. [PubMed: 17468748]
- Vazquez BY, Hightower CM, Martini J, Messmer C, Frienesenecker B, Corbels P, Tsai AG, Intaglietta M. Vasoactive hemoglobin solution improves survival in hemodilution followed by hemorrhagic shock. *Crit Care Med*. 2011; 39:1461–1466. [PubMed: 21336111]
- Wan J, Forsyth AM, Stone HA. Red blood cell dynamics: from cell deformation to ATP release. *Integrative biology: quantitative biosciences from nano to macro*. 2011; 3:972–981. [PubMed: 21935538]
- Wan J, Ristenpart WD, Stone HA. Dynamics of shear-induced ATP release from red blood cells. *Proceedings of the National Academy of Sciences of the United States of America*. 2008; 105:16432–16437. [PubMed: 18922780]
- Wang X, Lou N, Xu Q, Tian GF, Peng WG, Han X, Kang J, Takano T, Nedergaard M. Astrocytic Ca²⁺ signaling evoked by sensory stimulation in vivo. *Nature neuroscience*. 2006; 9:816–823. [PubMed: 16699507]
- Xie L, Kang H, Xu Q, Chen MJ, Liao Y, Thiyagarajan M, O'Donnell J, Christensen DJ, Nicholson C, Iliff JJ, et al. Sleep drives metabolite clearance from the adult brain. *Science*. 2013; 342:373–377. [PubMed: 24136970]
- Yacoub E, Shmuel A, Pfeuffer J, Van De Moortele PF, Adriany G, Ugurbil K, Hu X. Investigation of the initial dip in fMRI at 7 Tesla. *NMR in biomedicine*. 2001; 14:408–412. [PubMed: 11746933]
- Yoon YZ, Hong H, Brown A, Kim DC, Kang DJ, Lew VL, Cicuta P. Flickering analysis of erythrocyte mechanical properties: dependence on oxygenation level, cell shape, and hydration level. *Biophysical journal*. 2009; 97:1606–1615. [PubMed: 19751665]
- Zhou Y, Jia Y, Buehler PW, Chen G, Cabrales P, Palmer AF. Synthesis, biophysical properties, and oxygenation potential of variable molecular weight glutaraldehyde-polymerized bovine hemoglobins with low and high oxygen affinity. *Biotechnology progress*. 2011; 27:1172–1184. [PubMed: 21584950]
- Zhu X, Bergles DE, Nishiyama A. NG2 cells generate both oligodendrocytes and gray matter astrocytes. *Development*. 2008; 135:145–157. [PubMed: 18045844]

Highlights

- Activity-dependent cortical hyperemia begins in capillaries
- Transient dips in tissue O₂ tension drive capillary hyperemia
- Depletion of O₂ increases isolated erythrocyte flow velocity *ex vivo*
- Erythrocytes are O₂ sensors that regulate their own deformability and flow velocity

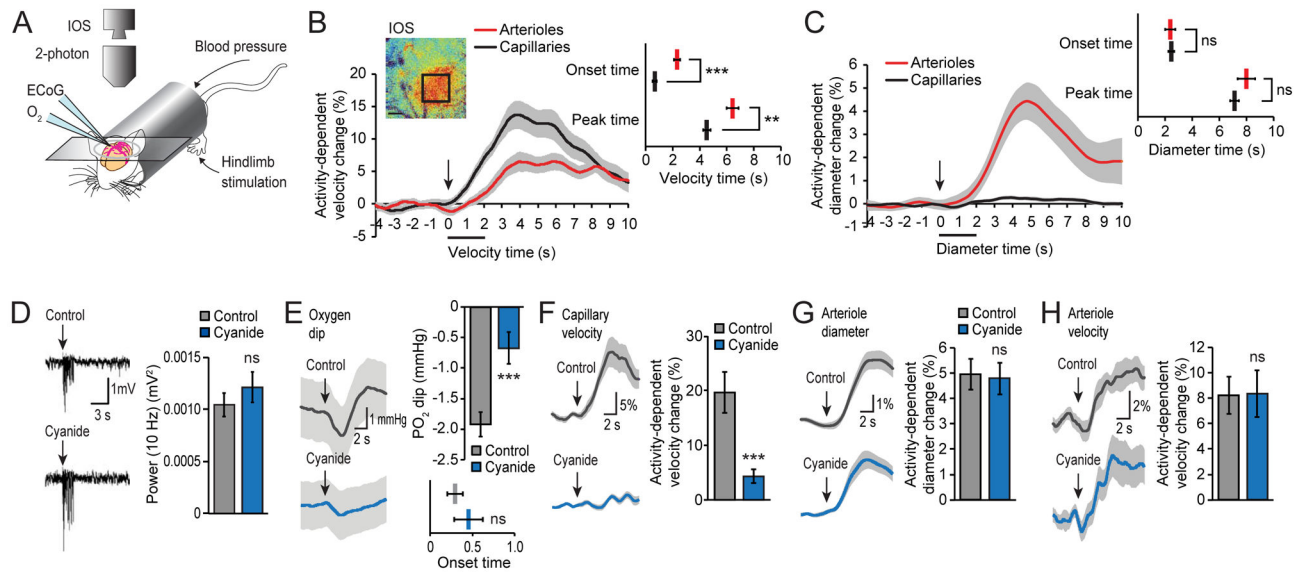


Figure 1. PO₂ Dips Are Necessary to Elicit Capillary Hyperemia, See also Figure S1

A. Experimental setup for assessing functional hyperemia elicited by sensory stimulation. Arterial blood pressure was monitored through a femoral artery catheter while the other hindlimb was stimulated. Through a cranial window, intrinsic optical signaling (IOS) was used to identify the cortical region of functional hyperemia. LFP and O₂ sensor microelectrodes were placed in close proximity (10–20 μm) to one another within the activated region. During hindlimb stimulation, blood vessels in the activated contralateral hindlimb cortex were imaged using two-photon laser scanning microscopy. **B.** Time-course plot of hindlimb stimulation-evoked RBC velocity changes in cortical arterioles (red) and capillaries (black). *Inset:* IOS imaging (shown as a pseudocolor image) was used to identify the location of the activated hindlimb cortex in all experiments. Scale bar, 300 μm. Evoked RBC velocity increases began in capillaries (0.67 ± 0.15 s) prior to arterioles (2.33 ± 0.22 s). $n = 61\text{--}65$, 25 mice. ***, $p < 0.001$, t-test; **, $p < 0.01$, Mann-Whitney test. Black arrow indicates start of stimulation, black bar indicates duration of stimulation. **C.** Time-course plot of diameter changes of cortical arterioles (red) and capillaries (black). Arterioles began to dilate at 2.38 ± 0.37 s and capillaries at 2.46 ± 0.22 s after hindlimb stimulation. $n = 53\text{--}283$, 15–18 mice. ns, $p > 0.05$, Mann-Whitney test. **D.** Topical treatment with cyanide (100 μM) did not alter LFP power within the duration of the experiments. $n = 13$, 5 mice. ns, $p > 0.05$, paired t-test. **E.** Activity-dependent PO₂ dips were suppressed by cyanide (1.92 ± 0.20 mmHg PO₂ dip without NaCN, 0.67 ± 0.26 mmHg PO₂ dip with NaCN). $n = 36\text{--}47$, 4–21 mice. ***, $p < 0.001$, Mann-Whitney test. Onset of the evoked PO₂ dip was unchanged by cyanide (0.29 ± 0.09 s without NaCN, 0.46 ± 0.17 s with NaCN). $n = 36\text{--}47$, 4–21 mice. ns, $p > 0.05$, Mann-Whitney test. **F.** Activity-dependent increases in capillary RBC velocity was nearly abolished by cyanide ($19.66 \pm 3.83\%$ without NaCN, $4.29 \pm 1.20\%$ with NaCN). $n = 29\text{--}38$, 6–13 mice. ***, $p < 0.001$, t-test. **G.** Activity-dependent penetrating arteriole vasodilation was unaffected by cyanide ($4.95 \pm 0.61\%$ without NaCN, $4.79 \pm 0.61\%$ with NaCN). $n = 66\text{--}79$, 13–17 mice. ns, $p > 0.05$, Mann-Whitney test. **H.** Activity-dependent increases in cortical arteriole RBC velocity persisted in the presence of cyanide (8.22

$\pm 1.47\%$ without NaCN, $8.36 \pm 1.85\%$ with NaCN). $n = 35-43$, 18–19 mice. ns, $p > 0.05$, Mann-Whitney test. Data are represented as mean \pm SEM.

Author Manuscript

Author Manuscript

Author Manuscript

Author Manuscript

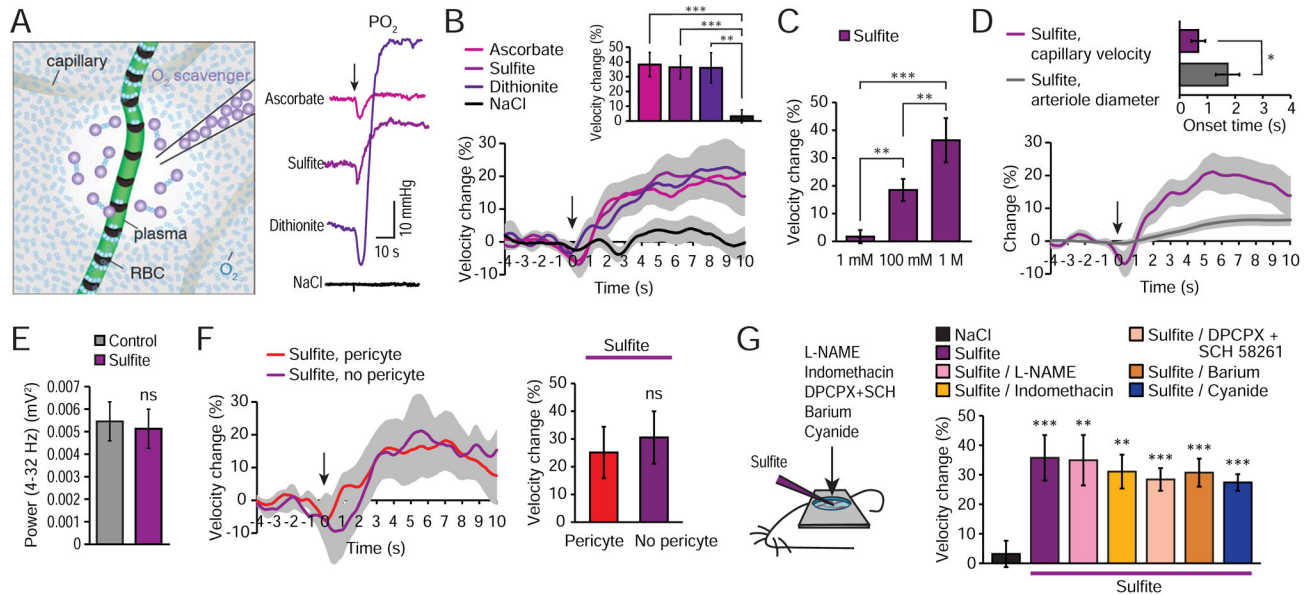


Figure 2. PO₂ Dips Are Sufficient to Elicit Capillary Hyperemia, See also Figure S2

A. Left: Experimental setup used to study the effect of local application of O₂ scavengers (sodium ascorbate, sulfite, or dithionite, 1 M). The O₂ scavengers were delivered by a micropipette inserted 100–150 μm below the pial surface and placed < 50 μm from a capillary. Upon microinjection, O₂ molecules within the vicinity of the pipette tip were trapped by the scavenger resulting in a transient drop in local O₂ tension. **Right:** Local tissue PO₂ was measured by an O₂ sensor placed < 50 μm from the scavenger pipette tip and displayed a transient reduction in O₂ tension followed by a PO₂ overshoot. Black arrow indicates time of microinjection. **B.** Nearby capillary RBC velocity increased robustly after microinjection of any of the O₂ scavengers: ascorbate, sulfite, or dithionite. **Inset:** A summary histogram of capillary RBC velocity changes induced by the transient reduction in tissue O₂ tension. n = 23–34, 6–12 mice. **, p < 0.01, ***, p < 0.001, Kruskal-Wallis with Dunn's test. **C.** Increasing the concentration of sulfite microinjected in close proximity to a capillary increased RBC velocity in a dose-dependent manner. n = 34–91, 4–12 mice. **, p < 0.01, ***, p < 0.001, Kruskal-Wallis with Dunn's test. **D.** Sulfite microinjection (1 M) near penetrating arterioles resulted in arteriole vasodilation that was delayed relative to capillary velocity increases. n = 19–34, 5–12 mice. *, p < 0.05, t-test. **E.** Sulfite microinjection (1 M) did not alter neuronal activity (LFPs) detected at a distance of < 50 μm from the sulfite pipette tip. n = 21, 4 mice. ns, p > 0.05, paired t-test. **F.** Local sulfite microinjection increased RBC velocity in both capillaries with pericytes and without pericytes identified in NG2-DsRed reporter mice. n = 5–8, 6 mice. ns, p > 0.05, t-test. Purple bar indicates sulfite microinjection groups. **G. Left:** Inhibitors were topically applied to the cranial window prior to microinjection of sulfite. **Right:** A summary histogram of capillary RBC velocity changes induced by sulfite microinjection in the presence of the nitric oxide synthase (NOS) inhibitor L-NAME (2 mM), cyclooxygenase (COX) inhibitor indomethacin (500 μM), adenosine receptor inhibitors DPCPX and SCH 58261 (each 1 μM), K⁺ channel inhibitor barium (100 μM), and cytochrome c oxidase inhibitor cyanide (100 μM). n = 27–

47, 5–6 mice. **, $p < 0.01$, ***, $p < 0.001$, compared to saline, Kruskal-Wallis with Dunn's test. Data are represented as mean \pm SEM.

Author Manuscript

Author Manuscript

Author Manuscript

Author Manuscript

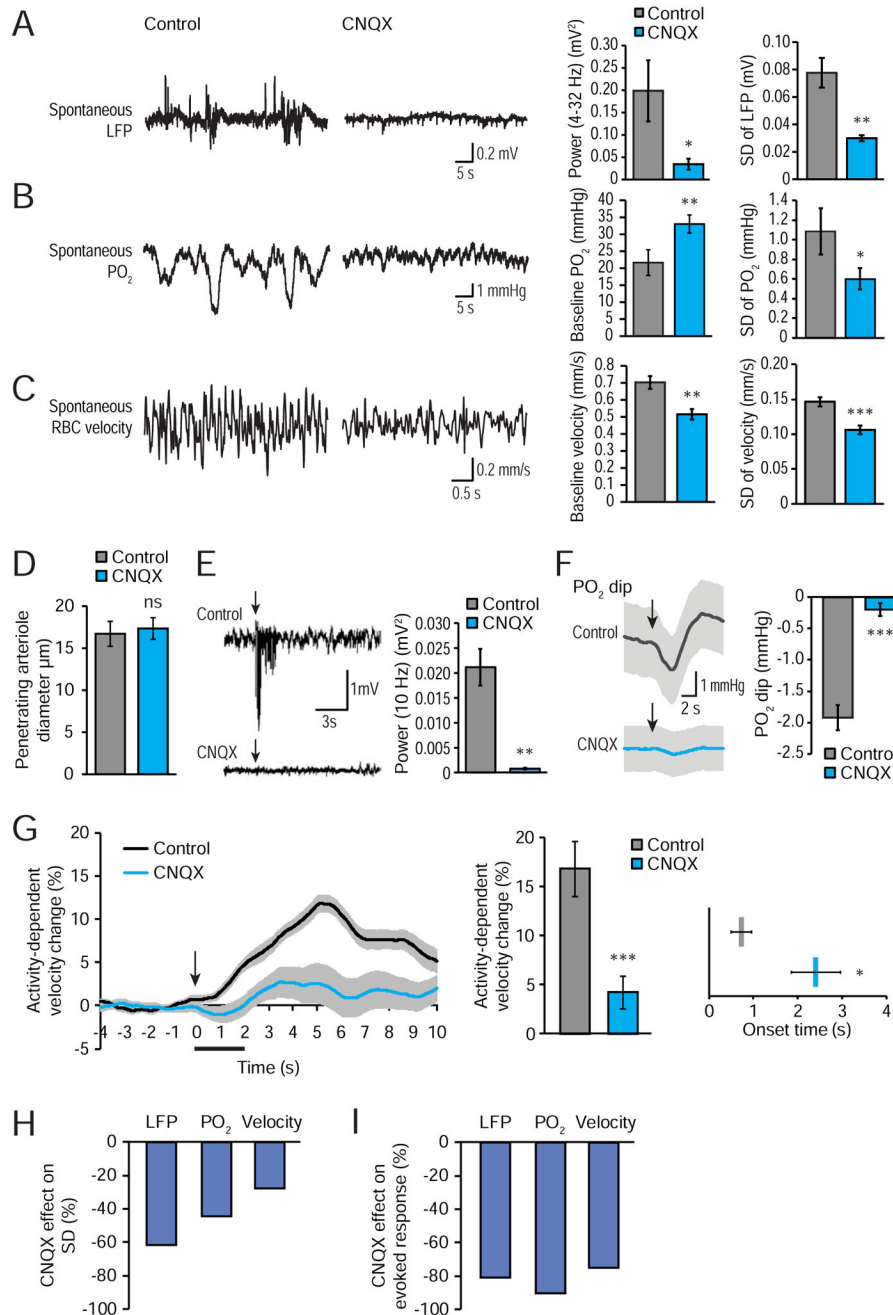


Figure 3. Capillary RBC Velocity Is Modulated by AMPA Receptor Activity, See also Figure S3
 The AMPA receptor inhibitor CNQX (200 μM) was added to the aCSF covering the cranial window for 30–45 minutes and recordings with and without CNQX were compared. **A.** Comparison of spontaneous (unstimulated) LFP activity (power at 4–32 Hz), as well as standard deviation of spontaneous LFP activity before and after CNQX. $n = 6$ mice. *, $p < 0.05$, **, $p < 0.01$, t-test. **B.** Comparison of baseline PO₂ level and the spontaneous variability (standard deviation) of PO₂ before (21.65 ± 3.77 mmHg baseline and 1.09 ± 0.24 mmHg SD) and after (33.03 ± 2.64 mmHg baseline and 0.60 ± 0.11 mmHg SD) CNQX. $n = 6$ –8 mice. **, $p < 0.01$, *, $p < 0.05$, paired t-test. **C.** Comparison of baseline capillary RBC

velocity and the spontaneous variability of RBC velocity before (0.70 ± 0.04 mm/s baseline and 0.15 ± 0.007 mm/s SD) and after (0.52 ± 0.03 mm/s baseline and 0.11 ± 0.006 mm/s SD) CNQX. $n = 131-191$, $12-13$ mice. **, $p < 0.01$, ***, $p < 0.001$, Mann-Whitney test. **D.** CNQX did not alter the baseline diameters of penetrating arterioles (16.71 ± 1.48 μ m before CNQX, 17.35 ± 1.28 μ m after CNQX). $n = 30$, 7 mice. ns, $p > 0.05$, Wilcoxon test. **E.** Comparison of excitatory potentials evoked by hindlimb stimulation quantified as the LFP power at 10 Hz before and after CNQX. $n = 15-23$, $3-4$ mice. **, $p < 0.01$, t-test. Black arrow indicates start of stimulation. **F.** Hindlimb stimulation-induced PO_2 dips were suppressed by CNQX (1.92 ± 0.20 mmHg in controls, 0.19 ± 0.10 mmHg after CNQX). $n = 29-47$, $9-21$ mice. ***, $p < 0.001$, Mann-Whitney test. **G.** Activity-dependent increases in capillary RBC velocity were reduced by CNQX. Bar histograms compare activity-induced capillary RBC velocity increases and onset times without ($16.76 \pm 2.76\%$ increase and 0.73 ± 0.23 s onset) and with ($4.19 \pm 1.68\%$ increase and 2.41 ± 0.56 s onset) CNQX. $n = 49-54$, $10-13$ mice. ***, $p < 0.001$, *, $p < 0.05$, Mann-Whitney test. Black arrow indicates start of stimulation, black bar indicates duration of stimulation. **H.** Suppression of spontaneous variability in LFPs, PO_2 , and capillary RBC velocity before and after CNQX as measured by standard deviation. **I.** Suppression of activity-induced changes in LFPs, PO_2 dip, and capillary RBC velocity by CNQX. Data are represented as mean \pm SEM.

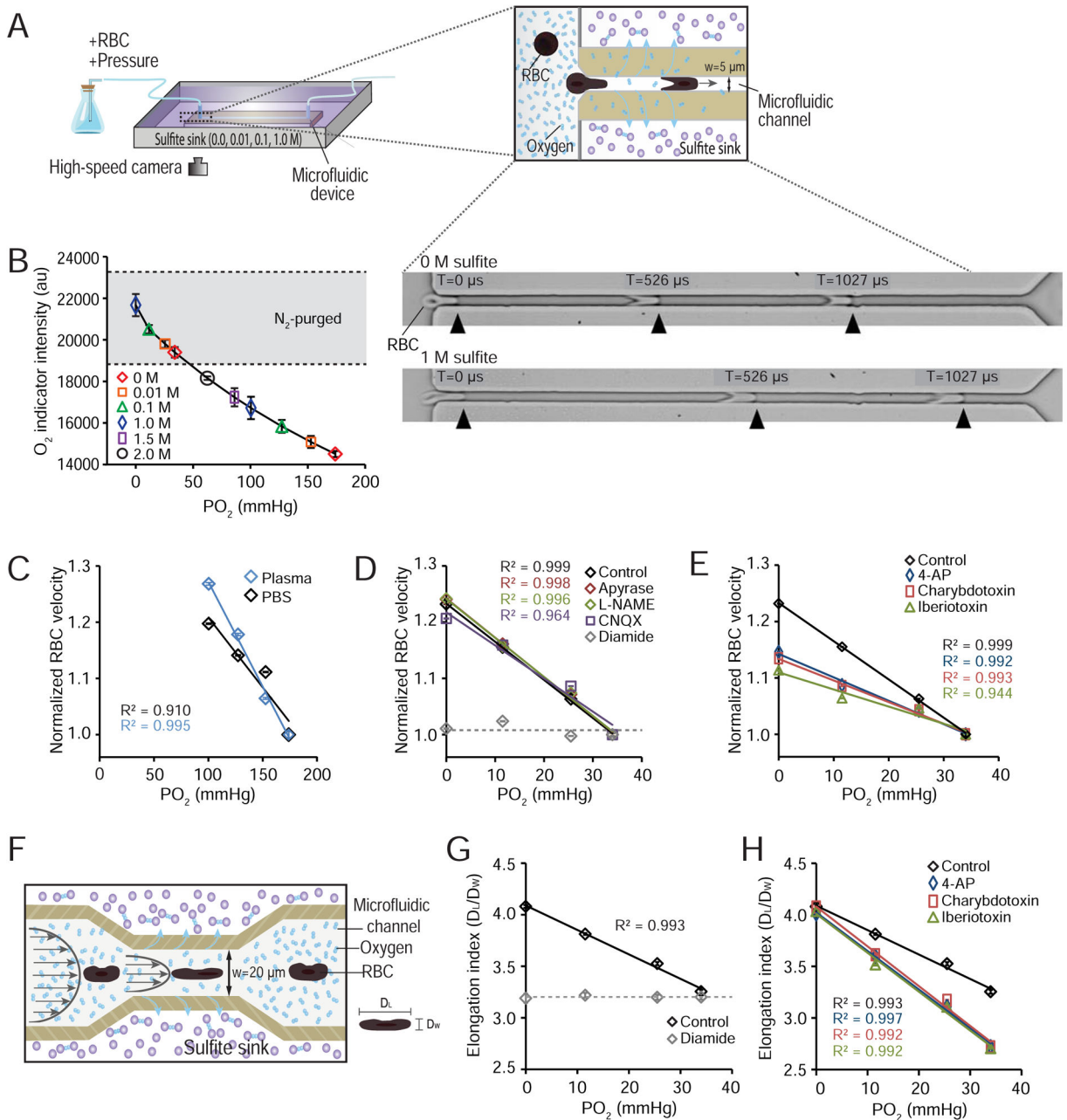


Figure 4. Oxygen Depletion Alone Is Sufficient to Increase RBC Velocity *ex vivo*

A. A diagram of the experimental setup for *ex vivo* analysis of the effect of PO₂ on RBC flow velocity. Human RBCs (~7 μ m in diameter) were added to the bath containing PBS and forced to flow through a microfluidic device containing a narrow channel (5 μ m) by applying a constant pressure (1.6 psi). The microfluidic device was submerged in an O₂ sink (chamber containing H₂O with 0.0, 0.01, 0.1, or 1.0 M sodium sulfite). PO₂ in the microfluidic channel was successively lowered by increasing the concentration of sulfite in the O₂ sink (0.0–1.0 M). RBC motion was captured by a high-speed camera. w: width. **B.** *Left:* To colorimetrically quantify PO₂ in the capillary channel, 25 μ M of tris(2,2'-

bipyridyl)dichlororuthenium(II) hexahydrate was prepared in N₂-bubbled deionized (DI) water (n = 3) and in air-saturated DI water (n = 4). The change in fluorescence intensity of the O₂ indicator dye solution flowing through the microfluidic device was measured during exposure to 0.0, 0.01, 0.1, 1.0, 1.5 and 2.0 M sodium sulfite solution and converted to PO₂. *Right:* Images comparing RBC flow within an O₂ sink containing 0 or 1 M sulfite. Images of flowing RBCs captured by the high-speed camera at sequential time points are superimposed. T: time. **C.** Lowering PO₂ in the microfluidic channel caused an increase in RBC velocity. Responsiveness of RBCs to surrounding PO₂ levels did not differ regardless of resuspension in PBS (n = 214, RBC velocity (mm/s) = $-0.137 \times \text{PO}_2 \text{ (mmHg)} + 80.056$, R² = 0.910) or plasma (n = 42, RBC velocity (mm/s) = $-0.157 \times \text{PO}_2 \text{ (mmHg)} + 69.069$, R² = 0.995). p > 0.05, t-test with Bonferroni test. **D.** The starting PO₂ in the PBS bath was lowered to 34 mmHg by N₂ purging prior to immersion in the O₂ sink, and RBC velocity continued to be sensitive to surrounding PO₂ changes (n = 71, RBC velocity (mm/s) = $-0.451 \times \text{PO}_2 \text{ (mmHg)} + 82.074$, R² = 0.999). Dephosphorylation of extracellular ATP by apyrase (40 U/ml) or inhibition of NOS and AMPA receptors by L-NAME (3 mM) and CNQX (200 μM), respectively, did not alter RBC velocity increases in response to lowering surrounding PO₂. n = 5–74. p > 0.05, one-way ANOVA. When diamide (200 μM) was added to stiffen RBC membranes, lowering PO₂ failed to increase RBC velocity compared to controls. n = 70–71. p < 0.0001, t-test. **E.** In the presence of the potassium channel inhibitors 4-aminopyridine (4-AP) (1 mM) (n = 199, RBC velocity (mm/s) = $-0.299 \times \text{PO}_2 \text{ (mmHg)} + 82.304$, R² = 0.992), charybdotoxin (100 nM) (n = 197, RBC velocity (mm/s) = $-0.278 \times \text{PO}_2 \text{ (mmHg)} + 82.277$, R² = 0.993), or iberiotoxin (100 nM) (n = 188, RBC velocity (mm/s) = $-0.213 \times \text{PO}_2 \text{ (mmHg)} + 78.011$, R² = 0.944), the sensitivity of RBC velocity to the change in PO₂ was reduced. n = 188–199. p < 0.05, one-way ANOVA. **F.** A schematic of the experimental setup for *ex vivo* analysis of the effect of PO₂ on RBC deformability. RBCs suspended in a N₂-purged PBS solution were injected into a microfluidic device containing a constriction (width = 20 μm) and constant pressure (1.6 psi) was applied. The microfluidic device was submerged in an O₂ sink similar to Fig. 4A, and RBC motion was captured by a high-speed camera. The deformability of RBCs was characterized by the elongation index D_L/D_W, where D_L and D_W represent the length and thickness of a RBC flowing through the constriction. **G.** The elongation index (D_L/D_W) of RBCs increased with a decrease in surrounding O₂ levels for control RBCs (n = 239, RBC D_L/D_W = $-0.0237 \times \text{PO}_2 \text{ (mmHg)} + 4.0886$, R² = 0.993). Compared to control RBCs flowing through the channel, diamide-treated (200 μM) RBCs did not deform significantly in response to changes in PO₂. n = 88–239. p < 0.0001, t-test. **H.** Elongation indexes (D_L/D_W) of control RBCs and RBCs treated with 4-AP (1 mM) (n = 276, RBC D_L/D_W = $-0.0373 \times \text{PO}_2 \text{ (mmHg)} + 4.0224$, R² = 0.997), charybdotoxin (100 nM) (n = 256, RBC D_L/D_W = $-0.0386 \times \text{PO}_2 \text{ (mmHg)} + 4.0795$, R² = 0.992), or iberiotoxin (100 nM) (n = 208, RBC D_L/D_W = $-0.0377 \times \text{PO}_2 \text{ (mmHg)} + 4.0085$, R² = 0.992) at different O₂ tensions are shown. n = 208–276. p < 0.05, one-way ANOVA.

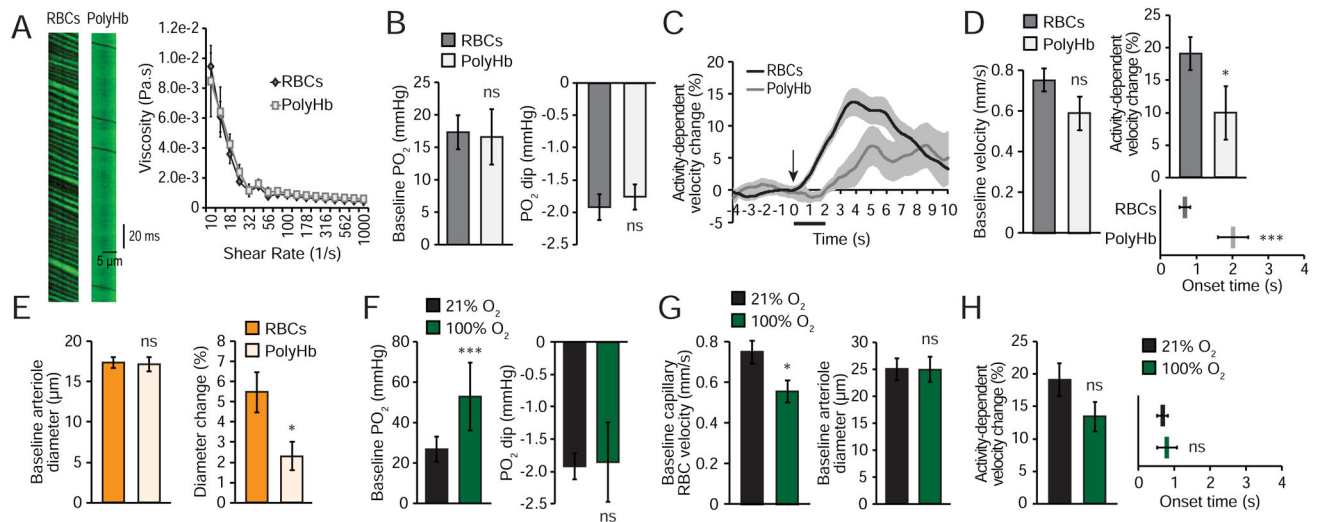


Figure 5. Oxygen Carriage by Erythrocytes Is Required for Functional Hyperemia

A. Left: Capillary line-scan images from a control and PolyHb-exchanged mouse. **Right:** PolyHb blood exchange does not alter blood viscosity. **B. Left:** Baseline tissue PO_2 is unchanged by PolyHb blood exchange (17.31 ± 2.62 mmHg in controls, 16.59 ± 4.27 in PolyHb). $n = 7-14$ mice. ns, $p > 0.05$, Mann-Whitney test. **Right:** PO_2 dip in response to hindlimb stimulation is similar between mice with and without PolyHb blood exchange (1.92 ± 0.20 mmHg PO_2 dip in controls, 1.76 ± 0.20 mmHg PO_2 dip in PolyHb). $n = 36-47$, $6-21$ mice. ns, $p > 0.05$, Mann-Whitney test. **C.** Capillary RBC velocity responses during hindlimb stimulation in mice with PolyHb blood replacement. Black arrow indicates start of stimulation, black bar indicates duration of stimulation. **D. Left:** Baseline capillary RBC velocity in mice with (0.59 ± 0.08 mm/s) and without (0.75 ± 0.06 mm/s) PolyHb blood exchange. $n = 23-65$, $8-25$ mice. ns, $p > 0.05$, Mann-Whitney test. **Right:** Comparison of capillary RBC velocity increases in response to hindlimb stimulation ($19.15 \pm 2.57\%$ in controls, $9.97 \pm 4.15\%$ in PolyHb). Onset time of capillary velocity changes (0.67 ± 0.15 s in controls, 2.02 ± 0.42 s in PolyHb). $n = 23-65$, $8-25$ mice. *, $p < 0.05$, Mann-Whitney test, ***, $p < 0.001$, t-test. **E. Left:** Baseline arteriole diameter in mice with (17.14 ± 0.85 μ m) and without (17.40 ± 0.68 μ m) PolyHb blood exchange. $n = 32-53$, $6-18$ mice. ns, $p > 0.05$, t-test. **Right:** % evoked arteriole vasodilation in mice with ($2.30 \pm 0.71\%$) and without ($5.47 \pm 0.99\%$) PolyHb blood exchange. $n = 32-53$, $6-18$ mice. *, $p < 0.05$, Mann-Whitney test. **F. Left:** Inspired 100% O_2 increases baseline brain parenchymal PO_2 (26.80 ± 6.24 mmHg PO_2 in room air, 52.89 ± 16.75 mmHg PO_2 in 100% O_2). $n = 15$ mice. ***, $p < 0.001$, Wilcoxon test. **Right:** Hindlimb stimulation-induced PO_2 dips were preserved in mice ventilated with 100% O_2 (1.92 ± 0.20 mmHg PO_2 dip in room air, 1.86 ± 0.61 mmHg PO_2 dip in 100% O_2). $n = 14-47$, $10-21$ mice. ns, $p > 0.05$, Mann-Whitney test. **G. Left:** Baseline capillary RBC velocity in mice ventilated with room air and 100% O_2 (0.75 ± 0.06 mm/s in room air, 0.56 ± 0.05 mm/s in 100% O_2). $n = 32-65$, $11-25$ mice. *, $p < 0.05$, Mann-Whitney test. **Right:** Baseline cortical arteriole diameter in mice ventilated with room air and 100% O_2 (24.96 ± 2.06 μ m in room air, 24.94 ± 2.34 μ m in 100% O_2). $n = 10$, 3 mice. ns, $p > 0.05$, paired t-test. **H. Left:** Hindlimb stimulation-evoked capillary RBC velocity increases ($19.15 \pm 2.57\%$ in room air, $13.44 \pm 2.25\%$ in 100% O_2). $n = 32-65$, $11-25$ mice. ns, $p > 0.05$, Mann-

Whitney test. *Right*: Onset time of capillary RBC velocity changes (0.67 ± 0.15 s in room air, 0.79 ± 0.27 s in 100% O₂). n = 32–65, 11–25 mice. ns, $p > 0.05$, Mann-Whitney test. Data are represented as mean \pm SEM.

Author Manuscript

Author Manuscript

Author Manuscript

Author Manuscript

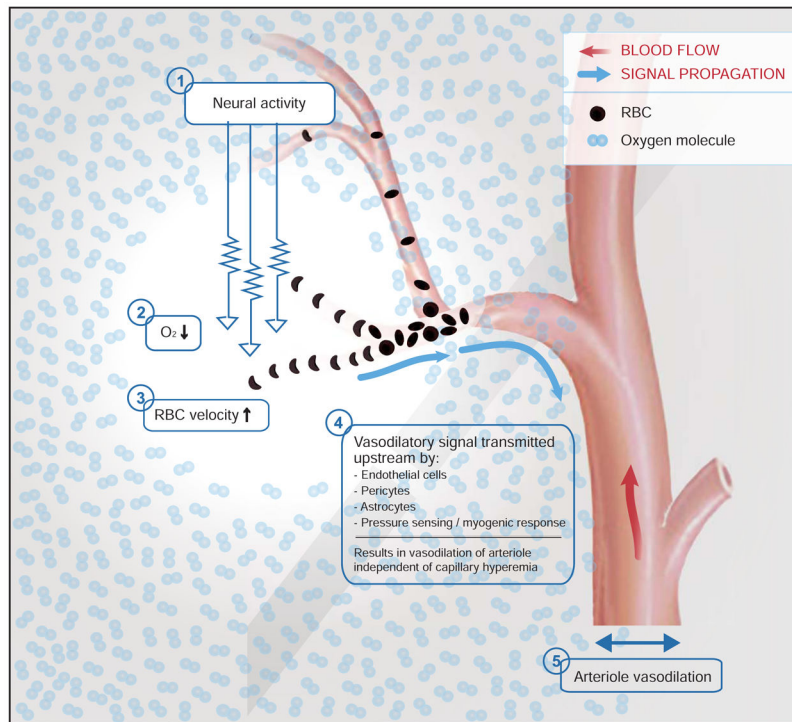


Figure 6. Model of Capillary Hyperemia and Potential Link to Upstream Arteriole Dilation (1) Sensory input triggers local neural activation resulting in (2) a local dip in tissue and plasma O_2 tension (Parpaleix et al., 2013). The dip in plasma O_2 tension changes the mechanical properties of RBCs resulting in (3) an increase in RBC velocity. The transient dip in O_2 tension drives the fast, initial phase of capillary hyperemia. The rise in RBC velocity in both capillaries and arterioles rapidly increases O_2 delivery resulting in an O_2 overshoot (4–5). The delayed and more sustained phase of capillary hyperemia is driven by vasodilation of upstream arterioles. It is not known whether the initial phase of capillary hyperemia, which is driven by a dip in local PO_2 , is mechanistically linked to the delayed dilation of the upstream arteriole. Hypothetical pathways of signal propagation along the neurovascular unit include Ca^{2+} signaling in endothelial cells, pericytes, or vascular endfeet of astrocytes. Also, it is possible that an initial increase in capillary perfusion results in pressure changes that trigger a myogenic response in the upstream arteriole. Finally, capillary hyperemia and arteriole vasodilation may be initiated independently. Several mechanisms, including release of vasoactive mediators from interneurons or astrocytes, are known to directly cause arteriole vasodilation (Cauli and Hamel, 2010; Iadecola and Nedergaard, 2007).